

See discussions, stats, and author profiles for this publication at: <https://www.researchgate.net/publication/331305168>

Design and Selection of Muscle Excitation Patterns for Modeling a Lower Extremity Joint Inspired Tensegrity

Conference Paper · February 2019

DOI: 10.1109/IRC.2019.00053

CITATIONS

5

5 authors, including:



Erik Jung

University of California, Santa Cruz

14 PUBLICATIONS 189 CITATIONS

[SEE PROFILE](#)

READS

1,125



Victoria T. Ly

University of California, Santa Cruz

4 PUBLICATIONS 21 CITATIONS

[SEE PROFILE](#)



Adam Buderi

University of California, Santa Cruz

1 PUBLICATION 5 CITATIONS

[SEE PROFILE](#)



Emma Appleton

University of California, Santa Cruz

1 PUBLICATION 5 CITATIONS

[SEE PROFILE](#)

Some of the authors of this publication are also working on these related projects:



Bio-inspired Tensegrity [View project](#)

Design and Selection of Muscle Excitation Patterns for Modeling a Lower Extremity Joint Inspired Tensegrity

Erik Jung¹, Victoria T. Ly¹, Adam Buderi¹,
Emma Appleton¹, and Mircea Teodorescu¹

Abstract— We propose a tensegrity-inspired design that emulates human lower extremity musculoskeletal connections as a network of rigid and tensile elements. Anatomical combinations of bones and muscles within joints provide structural stability, and manipulate configurations to maintain a standing position or enter a squat-like descent. We validated the predictions of our mathematical model with a computer simulation and a physical prototype. Bio-inspired joints controlled by muscle excitation patterns offers possibilities to revolutionize the innate flexibility within artificial limbs and future assistive devices.

I. INTRODUCTION

In nature, many skeletal-based systems inherently have the ability to manipulate physical stature and then return back to equilibrium in its relaxed position [1]. Designing a robust system with the characteristics of both sturdy, yet flexible is difficult. Systems consisting of rigid revolute joints (e.g., typically how the knee is modeled some robotic systems) cannot internally distribute forces similar to anatomical system. Rather when an outside force is introduced into a rigid system, this typically leads to stresses or fractures in the system [2].

However, rigid robotic systems are more predictable, which is advantageous when trying to understand the kinematics and dynamics of the entire system [3]. Within the many facets of types of robotics, there are passive and powered systems. The former is usually a system that consists of springs, or dampeners in order to disperse strain [4], [5] while powered systems require electric impulses in order to create movement [3], [6]. There exists both of these systems in soft and hard robotics which both demonstrate opposite attributes and qualities which handle stresses impacting the system differently [7]. A soft robotic system is better at adapting to an uncontrolled environment which could contain uneven terrain or unexpected forces while rigid systems preform better in a controlled and predictable environment, but these systems cannot usually carry a heavy load [5].

Tensegrity (“tensile with integrity”) [8] is considered to be a solution to the combination of hard and soft components. Tensegrity robotics ranges from robots created for exploration through rolling locomotion [9], [10], [11], to bio-inspired structures [12] and robotic systems that resemble different joints in the human skeleton [8], [13], [14], [15], [16].

This particular type of robotics consists of rigid and elastic elements which work in unison to return to equilibrium when acted upon by an outside force. The stresses distribute throughout the system (similar to that of a biological or soft robotic system) and can handle loads (much like a hard robotic system) due to the rigid and elastic elements that the system is comprised of. Notable human inspired actuated tensegrity structures are designs made to mimic the hip and knee joint [8] as well as shoulder and elbow joints [15], [16]. The previously mentioned shoulder and elbow joint evolved with tensegrity-inspired actuation strategies for a soft exosuit to assist stroke victims with rehabilitation for upper extremities [17].

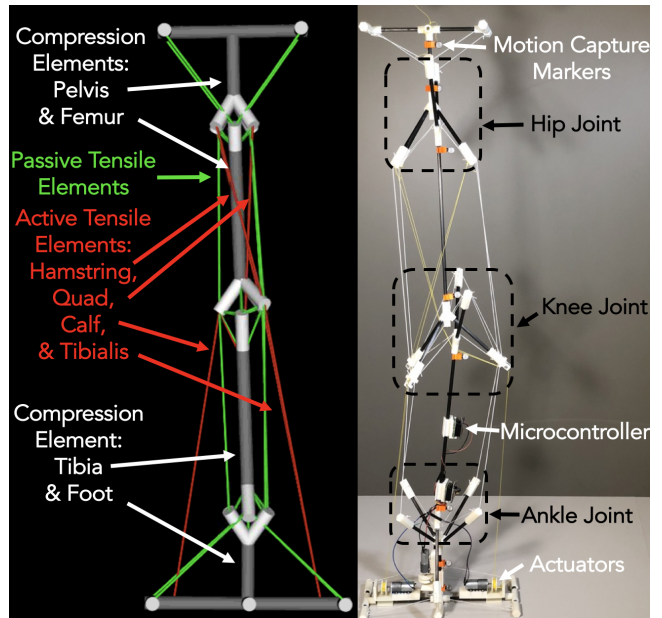


Fig. 1: (Left) Proposed lower extremity joint inspired tensegrity design in Simulation - OpenSim and (right) physical prototype. The passive elements are represented on the left in green and on the right in white. These passive elements can be thought of as ligaments in the body. The active cables are represented in red on the left. These can be loosely compared to muscles in the human body.

II. STRUCTURAL DESIGN & SIMULATION

A. Human Lower Extremity Inspired Joints

Musculoskeletal connections within the human body rely on the cohesive efforts between bones to support excess amounts of forces, and muscles and ligaments to manipulate

¹Dynamics Autonomous Navigation Surface Engineering and Robotics (DANSER) Lab at University of California Santa Cruz, Santa Cruz, CA 95064, USA ejung@ucsc.edu, vily@ucsc.edu, aabuderi@ucsc.edu, eappleto@ucsc.edu

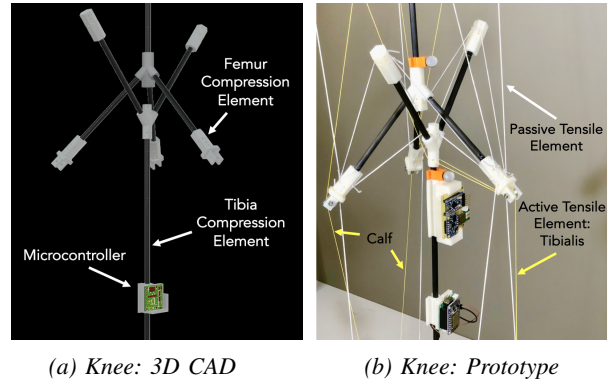
joints while maintaining poise. Tensegrity structures consists of rigid and elastic elements working in unison provide the structure with tensile integrity. When acted upon by an outside force, tensegrity structures are able to react and distribute the strain across other tensile forces, and return to a relaxed and fortified state. The lower half of the human body consists of many joints, in this paper we will centralize our focus towards mirroring the hip, knee and ankle joint in a forward axis enduring a squat-like descent.

The hip is capable of a variety of manipulated motions including adduction, abduction as well as extension. The knee joint flexes along one axis of rotation similar to revolute joints in rigid robotic systems. Plantar and dorsiflexion produced by the ankle joints also maintain innate flexibility to adhere to uneven terrain when performing gait [18]. Influenced by these three joints, we present a lower extremity tensegrity structure that is self-standing, and descends into a squat-like position.

1) Rigid Bodies: The lower extremity tensegrity structure in Figure 1 consists of rigid bodies, made with carbon fiber rods, located in the structure similar to the location of the pelvis (hip joint), femur (above the knee joint), tibia (below the knee joint) and foot (below the ankle joint). The hip and ankle joint are modeled in such a way through a tensegrity interlocked *Y-shape* and *quad-pronged* design to allow the joint have the freedom to move similar to a ball and socket joint but with more degrees of freedom (Figure 3a and 3b) . The knee joint is anatomically-modeled from the location of the patella as an extension from the femur. The knee, shown in Figures: 2a and 2b, have a slightly different configuration to the hip, where the knee consists of a set of interlocked *Y-shape* and *three-pronged* extrusions. These joints are surrounded by a network of passive elements that induces the structure with passive integrity, while allowing the structure to deform when introduced by a foreign force.

2) Tensile Components: Incorporating “muscles”, “fascia” and “ligaments” into our design implements elastic bungee cord (passive elements - influenced by tendons and ligaments) in conjunction with fishing-line spectra (active elements - muscles in the human body). Tensile elements provide the structure with innate stability and distribution for the joints and suspended the rigid bodies in a network keeping the system up-right. This lower extremity tensegrity structure is able to be actuated through the active tensile elements with the duality in the system similar to muscles: as one contracts the antagonistic pair releases to provide movement and less resistance. The passive tensile elements play a role to try to stabilize the system. Much like their active counterparts these elements also have antagonistic pairs, however, the passive elements distribute strain throughout the system and does not break due to the forces applied. Analyzing muscle activation patterns and locations in the lower extremities of the human body while preforming a squat, the active elements within the proposed tensegrity structure are routed in a similar manner [18], [19]. The motor driver drives the actuation strategies on the structure. Motors are located on the foot of the tensegrity structure (Figure

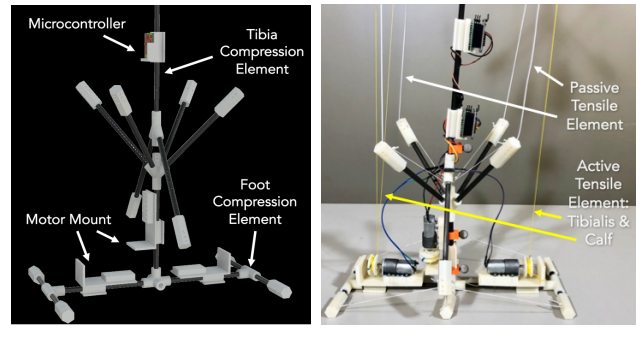
3a). Tightening the active elements on the rigid components (e.g., in order to ascend into the beginning of a squat), the tibialis and hamstring-inspired cables are relaxed creating an antagonistic contraction near the calf and quadriceps-inspired muscle.



(a) Knee: 3D CAD

(b) Knee: Prototype

Fig. 2: The knee joint proposed in the simulation environment is designed within the Fusion 360 CAD environment (a), then physical prototype (b).



(a) Ankle: 3D CAD

(b) Ankle: Prototype

Fig. 3: The ankle joint Fusion 360 CAD (a), and the physical prototype (b).

B. OpenSim Simulation

OpenSim is an open-source software that measures the dynamics of bio-mechanic systems by providing metrics such as joint angles, active forces, and passive forces. The OpenSim model proposed in this paper acts an extension of the suspended tensegrity model [8] with an additional ankle joint to perform a standing and squatting-inspired motion.

The bone class in OpenSim is a good analog for the rigid elements and the muscle and ligament classes represent the tensile elements.

The dependent muscle-inspired active tensile elements were placed as analogs to the tibialis, calf, hamstring and quadriceps (Figure 1). The active elements in the OpenSim model separate into two groups: the calf and quad as a pair of muscles controlling the downward descent, and the tibialis and hamstring a pair of muscles that drive the upward motion.

The *Thelen* muscle class characterize the active elements within the structure. The two calf muscles were placed to

pull the tibia body of the leg toward the ground while the tibialis muscles serve to pull the ankle back to an upright position. The two hamstring muscles were placed to keep the knee joint within its range of motion while leaning forward. Previous studies of muscle activation within human leg during a squatting motion confirm the placement and excitations of the muscles in the OpenSim model [18], [19]. The hip joint is kept within its range of motion by passive elements and does not need active actuation for the simulated experiment. Likewise, the lateral motion of the joints are restricted by the passive elements.

Within OpenSim each muscle class is influenced by the standard Hill equilibrium muscle model [20], and the muscle force outputs are a function of these factors:

- 1) p for level of activation values (%)
- 2) N^l for the normalized length of muscles (m)
- 3) N^T for normalized length of tendon (m)
- 4) N_v for normalized velocity of muscles (m/s)
- 5) θ for angular displacement (deg)
- 6) f_P for the passive force (N)
- 7) f_A represents the active force of the muscles (N)

Implementing this muscle group follows an equation for muscle-tension calculations to achieve the contracting and passive capabilities within the model [20].

$$\begin{aligned} \dot{N}^l &= N_v^{-1} N^T \left(\frac{f_P - f_P \cos(\theta)}{p(t) f_{AL}(N^l)} \right) \\ \dot{N}^l &= \frac{N_v^{-1} N^T}{N^l} \cdot \frac{f_P}{f_A} \cdot (p(t)(1 - \cos(\theta))) \end{aligned} \quad (1)$$

For simulating the motion of models without inputs external to the program, the Forward Dynamics (FD) tool interprets approximated muscle excitation, along with all other forces acting on the bodies of the model to simulate the physical behavior of the model in the simulated space. To validate a purely simulated motion of the leg, we compare the behavior of the physical prototype (Figure 7). The data from the simulation is a way to confirm the mechanics of the projected behavior of the lower extremity tensegrity structure. With this information, we can estimate kinematic behavior which can be applied to the physical tensegrity structure. FD models the acceleration and displacement of the coordinates of the OpenSim modeled leg as forces are applied to it via the muscles. The accelerations are found by integrating the model's musculoskeletal dynamical equations:

- 1) $\tau_m = [R(q)]f(a, l, \dot{l})$ for moment due to muscle forces
- 2) $\dot{l} = \Lambda(a, l, q, \dot{q})$ for muscle contraction dynamics
- 3) $\ddot{a} = A(a, x)$ for muscle activation dynamics

These equations root from the classical equations of motion [20] written together in the following form:

$$\ddot{x} = [W(x)]^{-1}(N + M(x, \dot{x}) + G(x) + F) \quad (2)$$

- 1) x for the vector of generalized positions
- 2) \ddot{x} for the vector of accelerations
- 3) \dot{x} for the vector of velocities
- 4) N for the vector of generalized forces
- 5) $[W(x)]^{-1}$ for the inverse of the mass matrix

- 6) $M(x, \dot{x})$ for the vector of Coriolis and centrifugal forces
- 7) $G(x)$ is the vector of gravitational forces
- 8) F is the vector for optional external forces applied to the model

s 5th-order Runge-Kutta-Feldberg integrator to solve for coordinate trajectories over the specified time interval in these dynamical equations [20]. The set of excitations found (Figure 6) resulted in a motion that was similar to the experimental data.

This form of calibration resulted in the combination of exertions that allow the tensegrity design to successfully stand, which led to the experimentation of initiating a squat. Running FD produced a motion that expresses the resulting simulated motion in terms of angles for each set of joints.

The Inverse Kinematics (IK) tool in OpenSim was used to analyze the recorded motion of the physical prototype. It matches a set of marker coordinates recorded over time from the leg in motion to markers on the model and calculates the closest approximation of each individual joint angle of the model to reproduce the motion in the simulation. Markers were placed on each compression element of the physical prototype. Identical markers were placed on the model in OpenSim to match the position of the physical markers. Mathematically, the closest approximation of joint angles is expressed as a weighted least squares problem that tries to minimize both marker and coordinate errors.

$$err_m = \sum_{u \in m} \omega_u \|z_u^{exp} - z_u(q)\|^2 \quad (3)$$

$$err_c = \sum_{l \in k} \tau_l (q_l^{exp} - q_l)^2 \quad (4)$$

$$\min_q [err_m + err_c] \quad (5)$$

where l and q is the vector of generalized coordinates being solved for, k stands for unprescribed coordinates, z_u^{exp} is the experimental position of marker u , $q_l = q_l^{exp}$ for all prescribed coordinates, m for markers coordinates, and q_l^{exp} is the experimental value for coordinate l , $x_u(q)$ is the position of the corresponding model marker (which depends on the coordinate values). ω and τ are marker and coordinate weights [20].

IK successfully produces a joint-angle-defined motion that approximates the motion of the physical prototype. Success in representing the prototype motion allows us to compare the behavior of the prototype to the behavior of the simulation behaving purely on its own.

III. PHYSICAL PROTOTYPE

The simulation approximates physical characteristics to approach angular displacements. Each programmable chip (ESP-12S module) is set up with WiFi compatibility and a motor driver that controls both the ankle and knee active elements shown at the base of Figure 1.

The ankle joint acts as a network host that receives commands from the controller, and reacts based from the assigned, θ_{target} , given by the user. The ankle joint focuses on

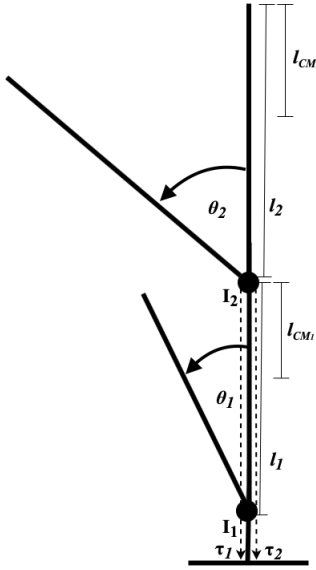


Fig. 4: Visual diagram of the mathematical model (Equation 7) representing the moment of inertia required to overcome by implementing the contraction of active tensile elements.

lateral movements, while the knee manipulates the muscle-inspired cables to create a squat-inspired downward and upward phase. Figure 4 focuses on angular displacements for the primary joints to descend: ankle θ_1 , and knee θ_2 .

$$y = \begin{bmatrix} \theta_1 \\ \theta_2 \end{bmatrix} = \begin{bmatrix} \theta_{\text{ankle}} \\ \theta_{\text{knee}} \end{bmatrix} = \begin{bmatrix} \theta_{\text{ankle}_x} & \theta_{\text{ankle}_y} & \theta_{\text{ankle}_z} \\ \theta_{\text{knee}_x} & \theta_{\text{knee}_y} & \theta_{\text{knee}_z} \end{bmatrix} \quad (6)$$

$$I[\theta] = \begin{bmatrix} c = m_2 l_1 l_{CM_2} & \\ [m_1 l_{CM_1}^2 + m_2 l_1^2 + I_1 & c \cdot \sin(\theta_1 - \theta_2)] \\ c \cdot \sin(\theta_1 - \theta_2) & m_2 l_{CM_2}^2 + I_2 \end{bmatrix}$$

$$M[\theta, \dot{\theta}] = \begin{bmatrix} 0 & c \cdot \cos(\theta_1 - \theta_2) \dot{\theta}_2 \\ -c \cdot \cos(\theta_1 - \theta_2) \dot{\theta}_1 & 0 \end{bmatrix}$$

$$G[\theta] = \begin{bmatrix} (m_1 l_{CM_1} + m_2 l_2) \cdot g \cdot \sin(\theta_1) \\ (m_2 l_{CM_2}) \cdot g \cdot \sin(\theta_2) \end{bmatrix}$$

$$U(\theta) = \begin{bmatrix} \tau_1 \tan(\theta_1) \\ \tau_2 \tan(\theta_2) \end{bmatrix}$$

$$I(\theta)\ddot{\theta} + M(\theta, \dot{\theta})\dot{\theta} + G(\theta) = U(\theta) \quad (7)$$

The structure's angular displacements are directly affected by the contraction of tensile forces from active muscle-inspired cables to overcome the moment of inertia, the coriolis and centrifuge forces with consideration of the effect of gravity (Equation 7) throughout upward or downward motion.

The $I(\theta)$ represents the inertial matrix, $M(\theta, \dot{\theta})$ represents the coriolis and centrifuge matrix, $G(\theta)$ represents the gravitational matrix, and U represents the acting tensile forces on the system with τ is the torque generated from the actuators. To characterize each segment (e.g., 3D fabricated pieces, PCB boards, carbon fiber rods), the required moment of inertia to overcome at each joint is approximated at the ankle and knee joints with inputs:

- 1) l_1 and l_2 for the length of both linkages

- 2) l_{CM_1} & l_{CM_2} for the length of the center of mass from the base of the linkage
- 3) m_1 & m_2 for the mass of each linkage
- 4) θ_1 for the angular displacement of the ankle
- 5) θ_2 for the angular displacement of the knee

TABLE I: Tensegrity Structure Characteristics

	$l[m]$	$l_{CM}[m]$	$m[kg]$	$I[kg \cdot m^2]$
Femur: 1	0.5766	0.2110	1.7744	0.1966
Tibia: 2	0.4064	0.3700	1.11	0.0611

The location of the muscles (Figure 1) on the front of the femur-based rigid body represent the quadriceps, or vastus medialis, and the back of the femur represents the biceps femoris, or hamstring. The tibia-based compression element mounts the tibialis in the front, and the calf on the back. The system off-centers the actuators towards the bottom to distribute weight near the ground limiting the rotational moment of inertia to overcome.

IV. RESULTS AND DISCUSSION

The combination of active and passive tensile elements manipulate the tensegrity-inspired design to maintain an upright position. The distribution of strain across the elastic elements within the joints allow the structure to follow a downward or upward kinematic pattern. The muscle activity measured with electromyographic (EMG) during the squat-like descent: is comparable to the experiments done by Dionisio et. al [18].

The main actuation strategies for the squat-like descent implements a wireless network with a WiFi host (i.e., ankle) and communicates to another microcontroller (i.e., knee) through User Datagram Protocol (UDP). The ankle interprets commands from the PC controller and either activates the motor driver on-board to manipulate the ankle-inspired tensile elements, or passes the command to the knee driver to contract and release the tibialis and calf-inspired components. The cable-driven actuators lengthen and relax the tibialis and hamstring muscles, while tightening the quadriceps and calf-inspired cables for a squat-like downward motion. Upon standing, the muscles work antagonistically to the previous where tibialis and hamstring-inspired muscles shorten bringing the leg to an upright position.

Muscle activation patterns, shown in Figure 5, represents the incremental trials tested to marginalize optimal values to achieve the squat-like descent. The under-approximated excitation results in little to no mechanical manipulation, whereas the over-approximated excitation caused the system

TABLE II: Effective range of motion comparison between human joints and tensegrity design [19].

Model	Joint	Lower Limit	Upper Limit
Tensegrity	Ankle	-30°	30°
	Ankle	-15°	40°
Tensegrity	Knee	-2.5°	90°
	Knee	0°	135°
Tensegrity	Hip	-20°	20°
	Hip	-20°	90°

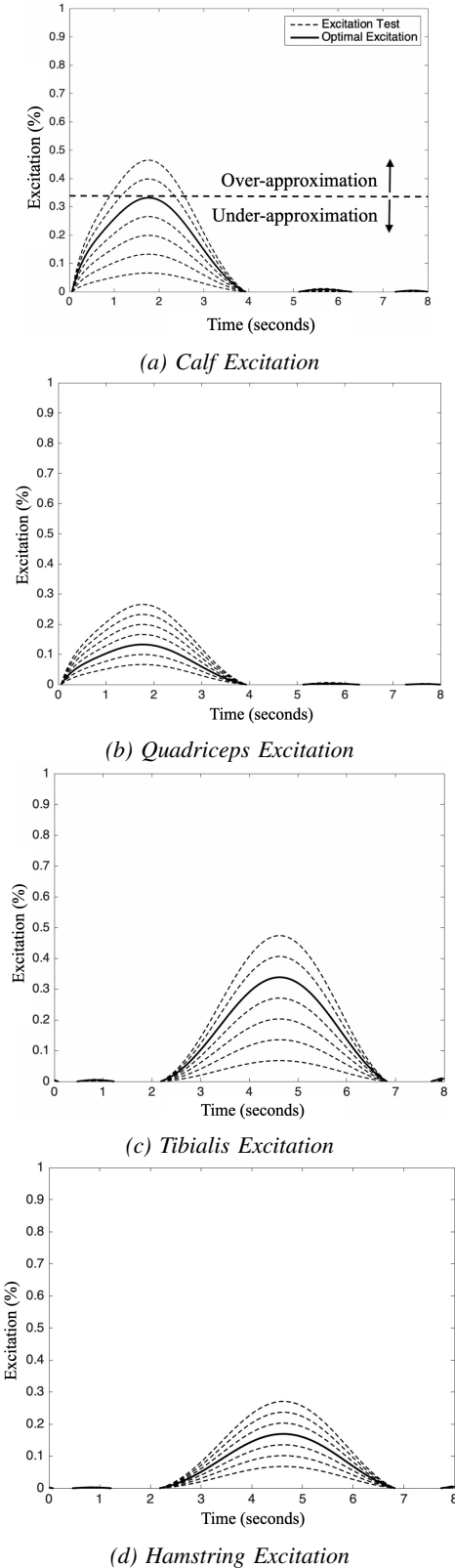


Fig. 5: Muscle activation patterns for a squat-like descent were increased incrementally 10% of the maximum to isolate the optimal excitation pattern. The undershoot (under the optimal line) is an under-approximation limiting the range of depth, while the overshoot (above the optimal line) to over-exertion causing the structure to fall over.

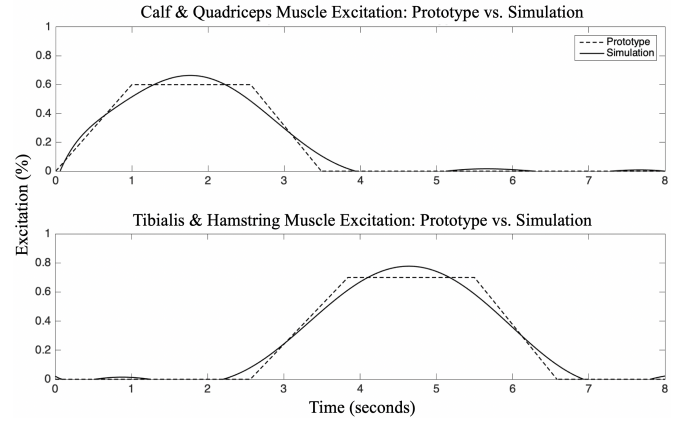


Fig. 6: Muscle excitation from the active elements, from the simulation, and the actuator PWM intensity are compared throughout the descending phase (1) and the standing phase (2).

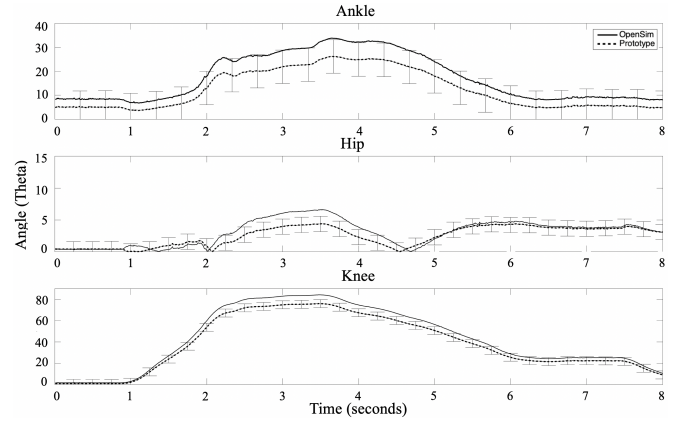


Fig. 7: Hip, knee, and ankle angular displacements of both the OpenSim simulation (dotted lines), and the motion capture of the physical prototype (solid lines) throughout the descent and standing phases. The error bars represent a selected amount (80-120% of optimal excitation) from simulated angular results.

to collapse or lead to unnatural behavior. Table II represents the angular displacement comparisons between the human and tensegrity model for the ankle, knee and hip joint.

OpenSim is used to understand the kinematic behavior during the squat-like descent that analyzes the pattern of muscles and ligaments to reach an ideal angle of anatomical relevance to a human leg. Actuators are driven by percentages of max current applied that mirrors the muscle activation shown in Figure 6. The optimal values, found through simulation, influence the contraction and relaxation patterns for the active elements, in the lower extremity tensegrity structure, to induce a squat-like descent. The experimental validation between the simulation and physical prototype (Figure 7) verify consistent behavior between accuracy with the simulation and the prototype.

V. CONCLUSION

The joints designed in this lower extremity tensegrity structure have the potential to revolutionize prostheses design for artificial lower limbs, due to their optimized anatomical equivalence of comfort for the users as well as more range

of motion more similar to that of the equivalent joint in the human biological system.

Implementing the OpenSim simulation environment validates range of motion and excitations between the proposed designs and human kinematic and EMG-reading behavior for muscle excitation patterns. Flexibility within models for the joints and muscles prove the potential ability of developing future tensegrity-inspired designs.

Tensegrity joints handle foreign external manipulations and can advance the load-bearing capabilities with different quality of actuation and materials. The implementation of physical prototypes focusing on structural integrity in an upright position proves the future of assistive wearable devices with tensegrity-based design in assistive devices is not far away.

REFERENCES

- [1] L. Nashner, "Adapting reflexes controlling the human posture," *Experimental brain research*, vol. 26, no. 1, pp. 59–72, 1976.
- [2] H. Springer Berlin Heidelberg, Martin, and et al, "Musculoskeletal robots and wearable devices on the basis of cable-driven actuators, soft robotics," pg. 42-53, 2015.
- [3] A. B. Zoss, H. Kazerooni, and A. Chu, "Biomechanical design of the berkeley lower extremity exoskeleton (bleex)," *IEEE/ASME Transactions On Mechatronics*, vol. 11, no. 2, pp. 128–138, 2006.
- [4] S. Krut, M. Benoit, E. Dombre, and F. Pierrot, "Moonwalker, a lower limb exoskeleton able to sustain bodyweight using a passive force balancer," in *Robotics and Automation (ICRA), 2010 IEEE International Conference on*, pp. 2215–2220, IEEE, 2010.
- [5] A. T. Asbeck, S. M. De Rossi, K. G. Holt, and C. J. Walsh, "A biologically inspired soft exosuit for walking assistance," *The International Journal of Robotics Research*, vol. 34, no. 6, pp. 744–762, 2015.
- [6] U. Onen, F. M. Botsali, M. Kalyoncu, M. Tinkir, N. Yilmaz, and Y. Sahin, "Design and actuator selection of a lower extremity exoskeleton," *IEEE/ASME Transactions on Mechatronics*, vol. 19, no. 2, pp. 623–632, 2014.
- [7] N. Costa and D. G. Caldwell, "Control of a biomimetic" soft-actuated" 10dof lower body exoskeleton," in *Biomedical Robotics and Biomechatronics, 2006. BioRob 2006. The First IEEE/RAS-EMBS International Conference on*, pp. 495–501, IEEE, 2006.
- [8] E. Jung, V. Ly, N. Cessna, L. Ngo, D. Castro, V. SunSpiral, and M. Teodorescu, "Bio-inspired tensegrity flexural joints," *Robotics and Automation (ICRA), IEEE International Conference*, 2018.
- [9] C. Paul, J. W. Roberts, H. Lipson, and F. V. Cuevas, "Gait production in a tensegrity based robot," in *Advanced Robotics, 2005. ICAR'05. Proceedings., 12th International Conference on*, pp. 216–222, IEEE, 2005.
- [10] Y. Koizumi, M. Shibata, and S. Hirai, "Rolling tensegrity driven by pneumatic soft actuators," in *Robotics and Automation (ICRA), 2012 IEEE International Conference on*, pp. 1988–1993, IEEE, 2012.
- [11] L.-H. Chen, K. Kim, E. Tang, K. Li, R. House, E. L. Zhu, K. Fountain, A. M. Agogino, A. Agogino, V. Sunspiral, et al., "Soft spherical tensegrity robot design using rod-centered actuation and control," *Journal of Mechanisms and Robotics*, vol. 9, no. 2, p. 025001, 2017.
- [12] D. Hustig-Schultz, V. SunSpiral, and M. Teodorescu, "Morphological design for controlled tensegrity quadruped locomotion," in *Intelligent Robots and Systems (IROS), 2016 IEEE/RSJ International Conference on*, pp. 4714–4719, IEEE, 2016.
- [13] E. Jung, V. Ly, D. Castro, and M. Teodorescu, "Knee-inspired tensegrity flexural joint," *Robotics and Automation (ICRA), IEEE International Conference*, 2018.
- [14] S. Lessard, J. Bruce, E. Jung, M. Teodorescu, V. SunSpiral, and A. Agogino, "A light-weight, multi-axis compliant tensegrity joint," *arXiv preprint arXiv:1510.07595*, 2015.
- [15] S. Lessard, D. Castro, W. Asper, S. D. Chopra, L. B. Baltaxe-Admony, M. Teodorescu, V. SunSpiral, and A. Agogino, "A bio-inspired tensegrity manipulator with multi-dof, structurally compliant joints," in *Intelligent Robots and Systems (IROS), 2016 IEEE/RSJ International Conference on*, pp. 5515–5520, IEEE, 2016.
- [16] L. B. Baltaxe-Admony, A. S. Robbins, E. A. Jung, S. Lessard, M. Teodorescu, V. SunSpiral, and A. Agogino, "Simulating the human shoulder through active tensegrity structures," in *ASME 2016 International Design Engineering Technical Conferences and Computers and Information in Engineering Conference*, pp. V006T09A027–V006T09A027, American Society of Mechanical Engineers, 2016.
- [17] S. Lessard, P. Pansodtee, A. Robbins, L. B. Baltaxe-Admony, J. M. Trombadore, M. Teodorescu, A. Agogino, and S. Kurianwan, "Crux: A compliant robotic upper-extremity exosuit for lightweight, portable, multi-joint muscular augmentation," in *Rehabilitation Robotics (ICORR), 2017 International Conference on*, pp. 1633–1638, IEEE, 2017.
- [18] V. C. Dionisio, G. L. Almeida, M. Duarte, and R. P. Hirata, "Kinematic, kinetic and emg patterns during downward squatting," *Journal of Electromyography and Kinesiology*, vol. 18, no. 1, pp. 134–143, 2008.
- [19] E. M. Arnold, S. R. Ward, R. L. Lieber, and S. L. Delp, "A model of the lower limb for analysis of human movement," *Annals of biomedical engineering*, vol. 38, no. 2, pp. 269–279, 2010.
- [20] SimTK, "How Forward Dynamics Works." <https://simtk-confluence.stanford.edu/display/OpenSim/How+Forward+Dynamics+Works>, 1993. [Online; accessed 25-August-2017].